

Tailoring Synthetic Polypeptide Design for Directed Fibril Superstructure Formation and Enhanced Hydrogel Properties

Tianjian Yang,[†] Tianrui Xue,[†] Jianan Mao, Yingying Chen, Huidi Tian, Arlene Bartolome, Hongwei Xia, Xudong Yao, Challa V. Kumar, Jianjun Cheng,* and Yao Lin*



Cite This: *J. Am. Chem. Soc.* 2024, 146, 5823–5833



Read Online

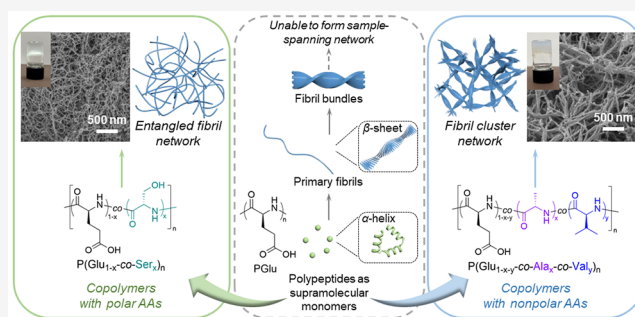
ACCESS |

Metrics & More

Article Recommendations

Supporting Information

ABSTRACT: The biological significance of self-assembled protein filament networks and their unique mechanical properties have sparked interest in the development of synthetic filament networks that mimic these attributes. Building on the recent advancement of autoaccelerated ring-opening polymerization of amino acid N-carboxyanhydrides (NCAs), this study strategically explores a series of random copolymers comprising multiple amino acids, aiming to elucidate the core principles governing gelation pathways of these purpose-designed copolypeptides. Utilizing glutamate (Glu) as the primary component of copolypeptides, two targeted pathways were pursued: first, achieving a fast fibrillation rate with lower interaction potential using serine (Ser) as a comonomer, facilitating the creation of homogeneous fibril networks; and second, creating more rigid networks of fibril clusters by incorporating alanine (Ala) and valine (Val) as comonomers. The selection of amino acids played a pivotal role in steering both the morphology of fibril superstructures and their assembly kinetics, subsequently determining their potential to form sample-spanning networks. Importantly, the viscoelastic properties of the resulting supramolecular hydrogels can be tailored according to the specific copolypeptide composition through modulations in filament densities and lengths. The findings enhance our understanding of directed self-assembly in high molecular weight synthetic copolypeptides, offering valuable insights for the development of synthetic fibrous networks and biomimetic supramolecular materials with custom-designed properties.



INTRODUCTION

The self-assembly of semiflexible protein filaments into networks through cross-linking or bundling is a ubiquitous phenomenon in biology, with examples including the cytoskeleton and collagen network.^{1–6} The mechanical properties of these filament networks hinge on the density of cross-links and the physical attributes of individual filaments. The interplay gives rise to distinct mechanical behaviors, such as viscoelasticity and mechanical plasticity that are often absent in synthetic polymeric gels.^{7–15} Therefore, there is significant interest in the design of synthetic filament networks that can mimic the fibrillarity and viscoelastic properties of biological gels. Specifically, materials derived from short peptides and polypeptides, prepared by solid-phase synthesis or recombinant technology, along with their amphiphilic variants, have greatly enhanced our understanding of the rational design of synthetic filament networks with the desired macroscopic properties.^{16–29}

High molecular weight (MW) synthetic polypeptides, produced via the ring-opening polymerization (ROP) of amino acid N-carboxyanhydride (NCA),^{30–34} have emerged as another promising candidate for developing bioinspired filament networks. Long regarded as model compounds for

proteins, these polypeptides can be synthesized on a large scale, making them cost-effective substitutes for biomaterial applications. Remarkably, even homopolymers of a single type of amino acid are capable of assembling into β -sheet nanofibrils in aqueous solutions under appropriate pH and temperature conditions.^{35,36} However, many such “simple” polypeptides either are incapable of forming supramolecular hydrogels or can do so only under highly specific conditions. To achieve successful hydrogel formation, rapid nanofibril entanglement or linkage is essential to generate a cohesive, sample-spanning network as opposed to precipitation. This constraint restricts their broader application as viscoelastic biomaterials. For example, under acidic conditions, poly(L-glutamic acid) (PGLu) forms amyloid-like fibrils that bundle into twisted ribbons.^{36–38} This transformation is driven by the thermodynamic tendency for aggregated fibrils to adopt

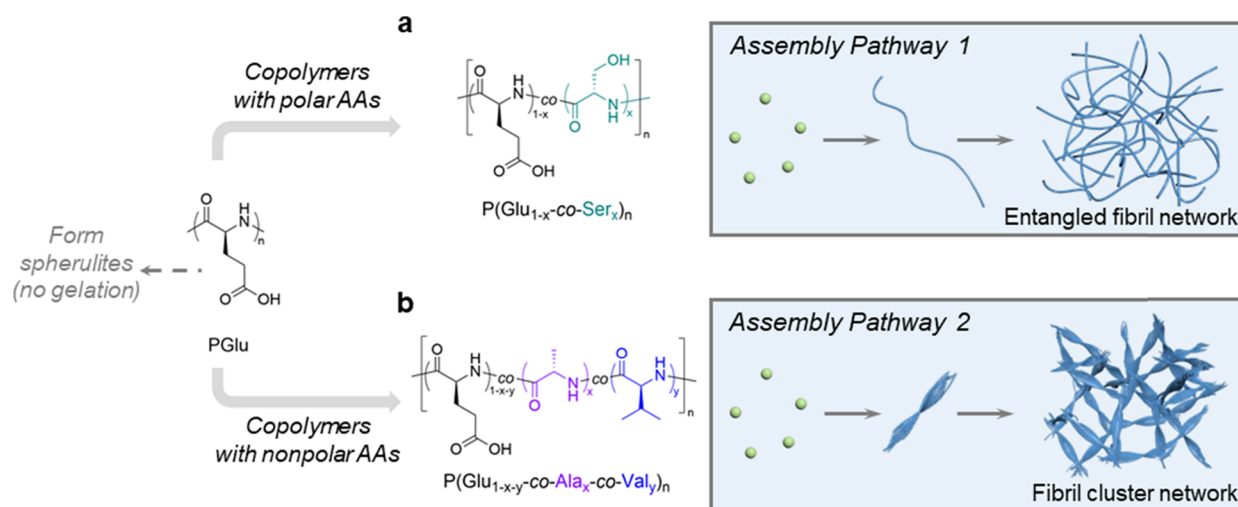
Received: September 29, 2023

Revised: December 16, 2023

Accepted: December 18, 2023

Published: January 4, 2024



Scheme 1. Illustration of the Two Supramolecular Hydrogelation Pathways Using Synthetic Random Copolypeptides Comprising Two or Three Different Amino Acids (AAs)⁴²


⁴²(a) Pathway 1 focuses on reducing fibril interaction potential, leading to a network of entangled long fibrils. (b) Pathway 2 centers on coupling enhanced β -sheet formation propensity with hydrophobicity, producing sample-spanning networks defined by interconnected fibril clusters.

pairwise orientation. Instead of progressing to gel states, these fibrils often crystallize into spherulite microparticles and precipitate.

Our aim is to elucidate the fundamental principles governing the networking pathways from nanofibrils of diverse interaction strengths and complex superstructures, diverging from the commonly employed amphiphilic assembly strategies.^{39,40} Gel formation, driven by the attractive forces between nanofibrils in concentrated suspension and subsequent percolation transitions, is an intricate nonequilibrium process.^{41–44} This process is shaped by an array of fibril characteristics, such as their aspect ratio, flexibility, tendency to bundle, entangle, or cross-link as well as the dynamics of fibril clustering and cross-link formation.^{41,45–49} Realizing sample-spanning networks with the desired mechanical properties demands extensive tunability of these parameters. In the realm of synthetic polypeptides, a promising tactic to address this challenge involves creating random copolymers that incorporate two or more distinct amino acids within single chains. The approach grants control over the self-assembly process, fibril properties, and network formation by adjusting the composition of copolypeptides. Given the vast chemical landscape provided by the 20 canonical amino acids, along with numerous unnatural amino acids,^{32,50,51} we can explore a diverse array of synthetic copolypeptides for the development of supramolecular hydrogels with tailored structures and properties.

Herein, we demonstrate that while certain homopolypeptides might be unable to form hydrogels on their own, their integration with other amino acids in random copolymers can lead to the development of supramolecular hydrogels with diverse fibril superstructures and mechanical properties. We selected glutamic acid (Glu) as the primary amino acid component in the copolymers given that PGlu itself cannot form a gel. We evaluated how the addition of one or two extra amino acids as comonomers, such as serine (Ser), leucine (Leu), valine (Val), tyrosine (Tyr), or alanine (Ala), could alter the fibril superstructure and gelation behavior of the copolypeptides. The recent advancement of autoaccelerated, cooperative covalent polymerization of NCAs has made it

possible to incorporate widely different amino acids in random copolymers while maintaining good control over the chemical composition and MWs.^{52–54} The process even accommodates amino acids like Ser, Val, and Tyr, which have a propensity to form β -sheets and are typically challenging to integrate using conventional methods.^{55–58} Leveraging this advanced technique, we successfully identified two distinct pathways that lead to supramolecular gelation of these random copolypeptides.

In the first approach, we designed the copolypeptide to have a fast fibrillation rate but a lower interaction potential among the formed fibrils. This allowed fibrils to remain relatively stable in suspension and entangle into homogeneous fibril networks at sufficiently high concentrations. Ser was found to be effective in facilitating supramolecular gelation over a broad composition range of the $P(\text{Glu}_{1-x}\text{-co-Ser}_x)_n$ copolymers (Scheme 1a), where n denotes the degree of polymerization (DP) and x and $1 - x$ denote the percentage composition of Ser and Glu, respectively. In the second approach, we explored the possibility of generating networks of branched fibril clusters by increasing the connectivity between the fibrils. Copolymers of Glu, Ala, and Val, $P(\text{Glu}_{1-x-y}\text{-co-Ala}_x\text{-co-Val}_y)_n$ (Scheme 1b), where x and y denote the percentage composition of Ala and Val, respectively, were found to form branched fibril clusters. Gelation occurred when the dynamics of the fibril clusters were arrested with network connectivity at appropriate concentrations. Fibril networks resulting from both pathways exhibited rheological properties of supramolecular gels, with considerable tunability in viscoelastic properties observed upon varying the composition of the copolypeptides.

RESULTS AND DISCUSSION

Synthesis of Diverse Copolypeptides as Supramolecular Monomers. We have designed a series of copolypeptides as supramolecular monomers with different compositions through the controlled ROP of NCAs. All of the NCA monomers we used in the study can be synthesized with high purity and scaled up effectively for copolymerization. The $P(\text{Glu}_{1-x}\text{-co-Ser}_x)_n$ copolymers were synthesized using the SIMPLE (Segregation-Induced Monomer-Purification and

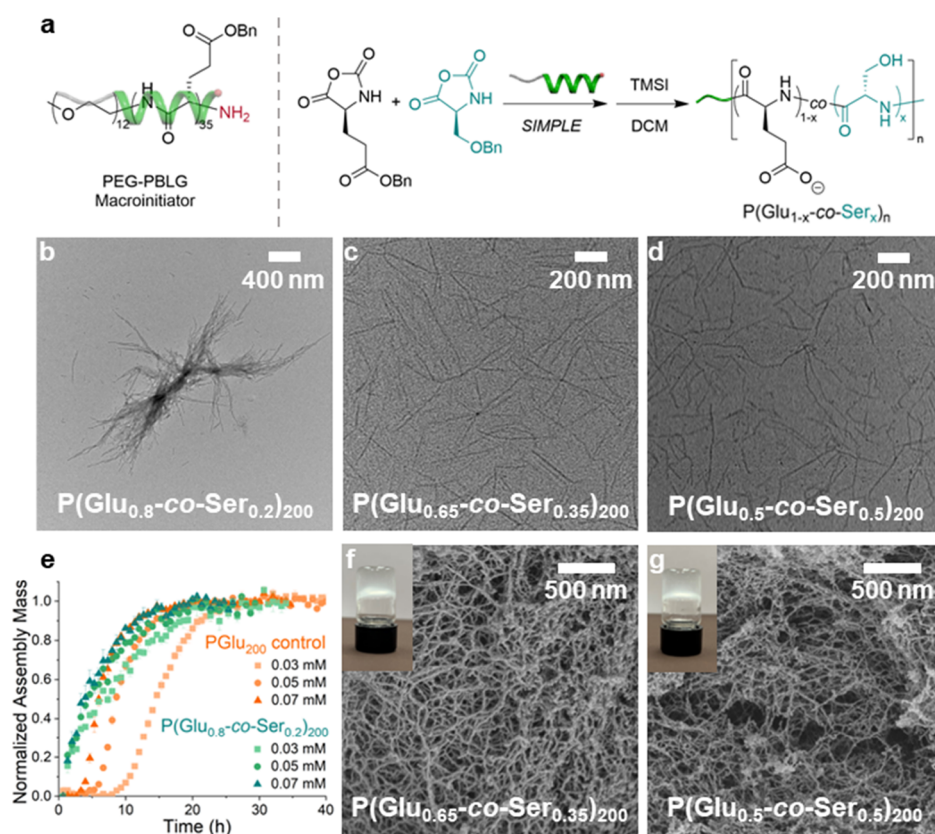


Figure 1. Synthesis and supramolecular assembly of $P(\text{Glu}_{1-x}\text{-co-Ser}_x)_n$ into long fibrils and entangled fibril networks. (a) Synthetic route of $P(\text{Glu}_{1-x}\text{-co-Ser}_x)_n$. (b) TEM image of the fibril bundles from $P(\text{Glu}_{0.8}\text{-co-Ser}_{0.2})_{200}$. (c, d) TEM images of the dispersed fibrils from $P(\text{Glu}_{0.65}\text{-co-Ser}_{0.35})_{200}$ and $P(\text{Glu}_{0.5}\text{-co-Ser}_{0.5})_{200}$, respectively. (e) Kinetic assembly profiles for $P\text{Glu}_{200}$ (in orange) and $P(\text{Glu}_{0.8}\text{-co-Ser}_{0.2})_{200}$ (in green) across different initial monomer concentrations. (f, g) SEM images of the entangled fibril networks from supercritical CO_2 dried hydrogels of $P(\text{Glu}_{0.65}\text{-co-Ser}_{0.35})_{200}$ and $P(\text{Glu}_{0.5}\text{-co-Ser}_{0.5})_{200}$, respectively. Inset: photographs of their translucent supramolecular hydrogels were taken at a concentration of 20 mg/mL.

initiator-Localization promoted rate-Enhancement) polymerization method initiated by the macroinitiator followed by iodotrimethylsilane (TMSI) deprotection.^{53,59} The $P(\text{Glu}_{1-x}\text{-co-Leu}_x)_n$ and $P(\text{Glu}_{1-x}\text{-co-Ala}_x)_n$ copolymers were synthesized from the DMF phase using hexylamine as the initiator using previously reported methods, followed by TMSI deprotection.⁶⁰ The $P(\text{Glu}_{1-x}\text{-co-Val}_x)_n$ and $P(\text{Glu}_{1-x}\text{-co-Tyr}_x)_n$ copolymers were synthesized from DCM phase using hexylamine as initiator using previously reported methods, followed by TMSI deprotection.^{61,62} The $P(\text{Glu}_{1-x-y}\text{-co-Ala}_x\text{-co-Val}_y)_n$ copolymers were synthesized from crown ether (CE) catalyzed polymerization method, followed by TMSI deprotection.⁶³ All the copolymers have similar degree of polymerization ($\text{DP} \sim 100$ or 200), low polydispersity ($\mathcal{D} < 1.1$), and precise composition control. Detailed synthesis and characterization of the corresponding macromolecules are shown in the Supporting Information (Figures S2–8, Table S1, and Figure S35–48).

Exploring the Role of Serine in the Rapid Formation of Entangled Fibril Networks. We first focused on developing long fibrils from copolypeptides that remain stable when diluted but transition into entangled fibril networks as the concentration increases. Serine (Ser) was selected owing to its distinct polar side chains and its propensity toward β -sheet formation. This exploration into entangled fibril network was motivated by the observed gelation characteristics of poly(L-lysine) (PLys). Unlike PGLu and most homopolypeptides, PLys can transform into hydrogels, consisting of elongated

nanofibrils, when the side-chain charges neutralize under alkaline conditions (Figure S1). This transformation is notably rapid and devoid of the typical nucleation lag phases often seen in amyloid-like supramolecular assemblies.^{37,64} Given Ser's propensity for β -sheet structures^{65–68} and its increased hydrophilicity compared to Glu in acidic environments⁶⁹ where self-assembly occurs, it is anticipated to act as a catalyst in the formation of widespread, elongated fibrils. At sufficiently high concentrations, these copolypeptide fibrils are likely to intertwine swiftly to form a sample-spanning network, overcoming the stacking challenges of PGLu fibrils and offering a cohesive and stable hydrogel structure, circumventing precipitation constraints.

We synthesized three $P(\text{Glu}_{1-x}\text{-co-Ser}_x)_{200}$ samples with increasing percentages of Ser ($x = 0.2, 0.35$ and 0.5) using autoaccelerated ROP-NCA in a water/dichloromethane (DCM) biphasic system with macroinitiators (SIMPLE polymerization), according to the procedures reported previously^{53,59} (Figure 1a and Figure S2–3). The statistical randomness of Glu and Ser incorporation into the copolymer chains was confirmed by monitoring the monomers consumption kinetics during the copolymerization (Figure S9). The copolypeptides, similar to PGLu, experienced a conformation shift from coil to helix when the pH was decreased from neutral to acidic, resulting in the suppression of carboxylate ionization (Figure S10). Under mild heating conditions that destabilize α -helices, aggregated β -structures

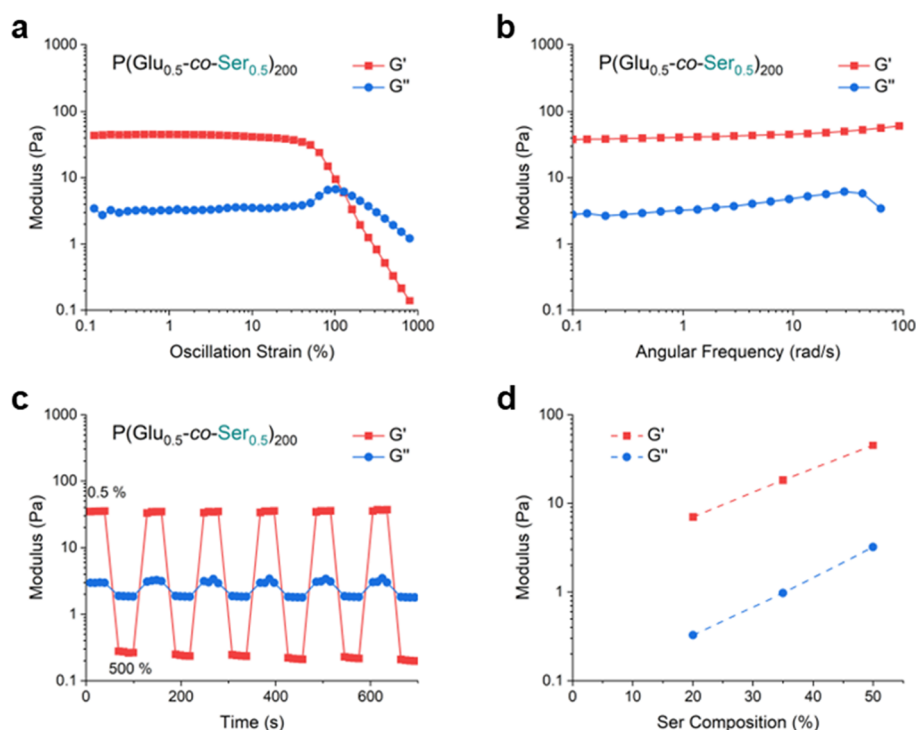


Figure 2. Rheological characteristics of hydrogel networks of entangled copolypeptide fibrils. (a) Strain-dependent oscillatory rheology for the $P(\text{Glu}_{0.5}\text{-co-Ser}_{0.5})_{200}$ hydrogel, conducted at $\omega = 1.0$ rad/s and 25°C . (b) Frequency-dependent oscillatory rheology for the $P(\text{Glu}_{0.5}\text{-co-Ser}_{0.5})_{200}$ hydrogel under 0.5% strain at 25°C . (c) Oscillatory rheology $P(\text{Glu}_{0.5}\text{-co-Ser}_{0.5})_{200}$ hydrogel showcasing self-healing properties when alternated between 0.5 and 500% strain over 30-s intervals at $\omega = 1.0$ rad/s and 25°C . (d) Comparison of storage and loss modulus for $P(\text{Glu}_{1-x}\text{-co-Ser}_x)_{200}$ supramolecular networks based on varying Ser compositions in the copolymer, measured under 1.0% strain, $\omega = 1.0$ rad/s, and 25°C . Polymer concentration is maintained at 20 mg/mL.

typically form as they maximize local contacts, rendering them thermodynamically more stable than α -helices. We selected the fibrillation condition of pH 4.0 and 45°C , commonly used in previous studies,^{36–38} to investigate the impact of varying Ser compositions on the fibrillation process.

The transmission electron microscopy (TEM) images presented in Figure 1b–d illustrate the fibril morphology from three $P(\text{Glu}_x\text{-co-Ser}_{1-x})_{200}$ samples, prepared in water with the pH adjusted to 4 using HCl. At a Ser content of 20%, $P(\text{Glu}_{0.8}\text{-co-Ser}_{0.2})_{200}$ formed loose fibril bundles (Figure 1b), which were distinct from tightly stacked, ribbon-like structure assembled from PGLu (Figure S1). The introduction of more hydrophilic Ser in the copolypeptide lowered the interaction potential among the formed fibrils, resulting in fibrils with a less tendency to assume pairwise orientation. As the Ser content reached 35% or 50%, most fibrils remained individually dispersed, with an average width of ~ 10 nm and a length of hundreds of nanometers (Figure 1c,d). Fourier-transform infrared spectra (FTIR) and wide-angle X-ray diffraction (WAXD) of the fibrils revealed that they were primarily composed of β -sheet structures (Figure S16 and S17). The kinetics of fibrillation were examined using thioflavin T (ThT)^{37,70} in a 15 mM acetate buffer (pH 4), monitoring the enhanced fluorescence emission upon ThT's binding to β -sheet structures. TEM analysis confirmed that the fibril morphologies remained consistent in the presence of an acetate buffer (Figure S23). Unlike the slow, nucleation-controlled assembly of PGLu, the copolypeptides, such as $P(\text{Glu}_{0.8}\text{-co-Ser}_{0.2})_{200}$ even in diluted solutions, displayed no initial lag phase—a stage typically marked by slow nucleation prior to rapid fibril growth—as shown in Figure 1e. The kinetic

rate of fibrillation accelerated with an increasing Ser percentage (Figure S22), attributable to the reduced charge repulsion and enhanced β -sheet propensity within the copolymers.

In a more concentrated solution (e.g., 20 mg/mL), $P(\text{Glu}_{0.8}\text{-co-Ser}_{0.2})_{200}$ remained as fibril suspensions (inset of Figure S31a). In contrast, $P(\text{Glu}_{0.65}\text{-co-Ser}_{0.35})_{200}$ and $P(\text{Glu}_{0.5}\text{-co-Ser}_{0.5})_{200}$ formed hydrogels within 30 min (insets of Figure 1f,g). The scanning electron microscopy (SEM) images showed that the hydrogels of both samples were made of an entangled supramolecular fibril network (Figure 1f,g). The fibrils in the networks had a similar width as the dispersed fibrils found in the diluted suspension. The viscoelastic properties of these supramolecular gels were then characterized by shear rheology.

Assessing and Tuning the Mechanical Properties of $P(\text{Glu}_{1-x}\text{-co-Ser}_x)_{200}$ Hydrogels. We examined the storage modulus (G') and loss modulus (G'') as functions of oscillatory strain and frequency for the $P(\text{Glu}_{0.5}\text{-co-Ser}_{0.5})_{200}$ hydrogels, as shown in Figure 2a–c. Within these hydrogels, G' was substantially higher than G'' , and negligible frequency dependence was observed, thus indicating their predominantly elastic nature. Figure 2a shows the results of the strain-dependent oscillatory rheology. The hydrogel made from $P(\text{Glu}_{0.5}\text{-co-Ser}_{0.5})_{200}$ demonstrated a G' of 40 Pa and sustained this value up to strains nearing $\sim 50\%$. Remarkably, in step-strain experiments—where a high strain (500%) was introduced after a low strain (0.5%) to perturb the hydrogel network and followed by another low strain to assess the network's recovery—this hydrogel demonstrated impressive self-healing abilities (Figure 2c). The G' of $P(\text{Glu}_{0.5}\text{-co-Ser}_{0.5})_{200}$ returned to approximately 100% of its initial value

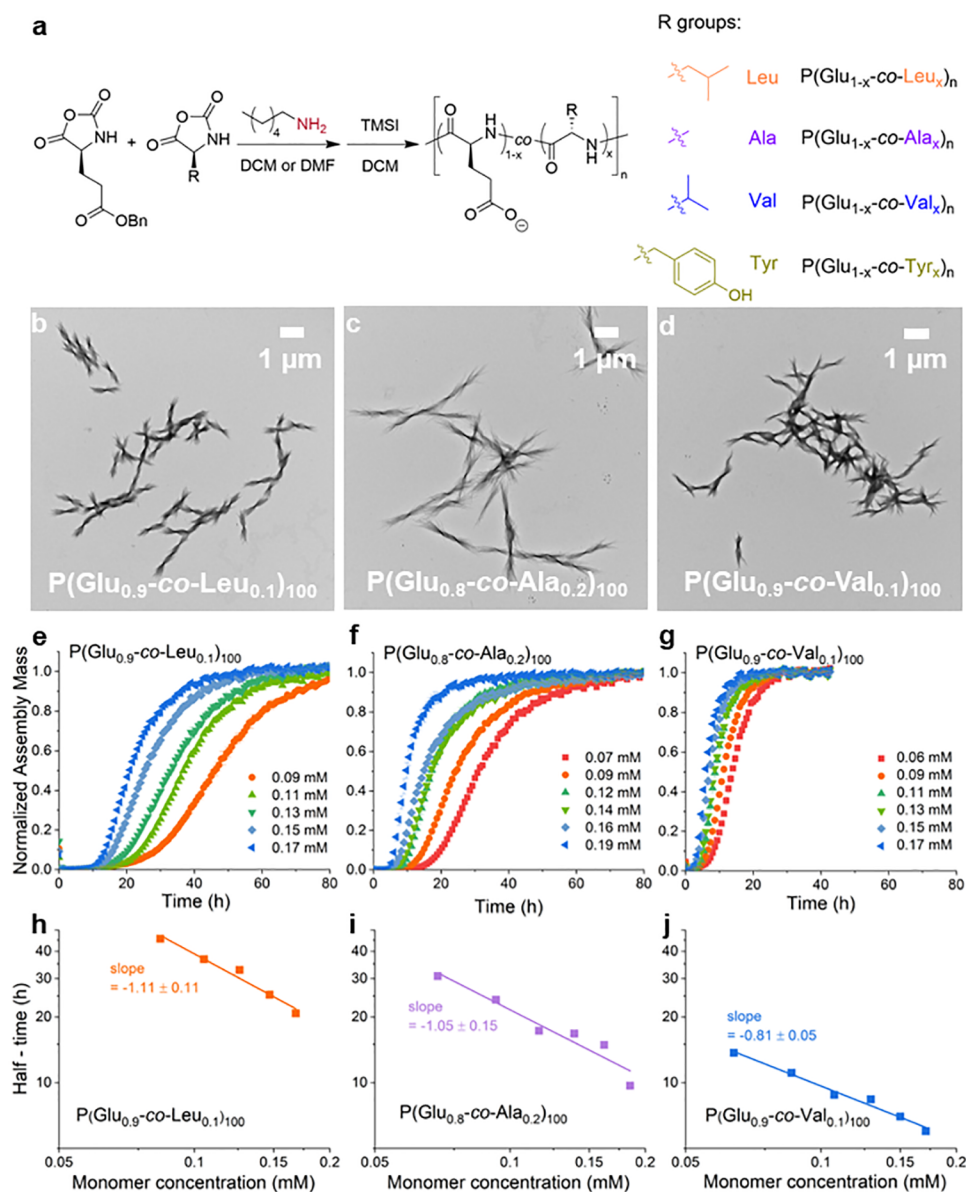


Figure 3. Supramolecular assembly of bicomponent random copolypeptides incorporating hydrophobic secondary amino acids. (a) Schematic representation of the synthetic routes of $P(\text{Glu}_{1-x}\text{-co-Leu}_x)_n$, $P(\text{Glu}_{1-x}\text{-co-Ala}_x)_n$, $P(\text{Glu}_{1-x}\text{-co-Val}_x)_n$, and $P(\text{Glu}_{1-x}\text{-co-Tyr}_x)_n$. (b–d) TEM images of the supramolecular fibril clusters for $P(\text{Glu}_{0.9}\text{-co-Leu}_{0.1})_{100}$, $P(\text{Glu}_{0.8}\text{-co-Ala}_{0.2})_{100}$, and $P(\text{Glu}_{0.9}\text{-co-Val}_{0.1})_{100}$, respectively. (e–g) Kinetic assembly profiles for $P(\text{Glu}_{0.9}\text{-co-Leu}_{0.1})_{100}$, $P(\text{Glu}_{0.8}\text{-co-Ala}_{0.2})_{100}$, and $P(\text{Glu}_{0.9}\text{-co-Val}_{0.1})_{100}$, respectively, across a range of initial monomer concentrations. (h–j) Power-law scaling of the time to half-completion ($t_{1/2}$) as a function of the initial monomer concentration during the assembly of $P(\text{Glu}_{0.9}\text{-co-Leu}_{0.1})_{100}$, $P(\text{Glu}_{0.8}\text{-co-Ala}_{0.2})_{100}$, and $P(\text{Glu}_{0.9}\text{-co-Val}_{0.1})_{100}$, respectively. Data points (represented by solid squares) were subjected to linear regression analysis (depicted by solid lines) to determine the slope that corresponds to the scaling exponent.

within seconds after the removal of high strain. By varying the Ser composition, we can tune the hydrogel's properties. For instance, the supramolecular hydrogel produced from $P(\text{Glu}_{0.65}\text{-co-Ser}_{0.35})_{200}$ (Figure S32) exhibited a softer gel compared to the $P(\text{Glu}_{0.5}\text{-co-Ser}_{0.5})_{200}$. Conversely, $P(\text{Glu}_{0.8}\text{-co-Ser}_{0.2})_{200}$ resulted in a viscous solution (Figure S31). The comparison among the three variants is showcased in Figure 2d.

While the $P(\text{Glu}_{1-x}\text{-co-Ser}_x)_{200}$ samples exemplify the tunable and reversible nature of supramolecular gels based on the entanglement of elongated dispersed fibrils, such dynamic attributes may also compromise their mechanical robustness. To address this, we subsequently pursued a

strategy to bolster the noncovalent network connections by incorporating nonpolar amino acids known for their strong β -sheet-forming propensity into the copolypeptides. This modification gives rise to superstructures of stiff, branched fibril clusters that can rapidly coalesce into a cohesive, sample-spanning network, thereby offering the potential for enhanced mechanical strength.

Diversifying Fibril Superstructures with Hydrophobic Amino Acid Integration. We utilized the ROP of NCA to synthesize a diverse set of copolypeptides, with Glu as the primary component and varying amounts of Leu, Val, Ala, or Tyr. Among these amino acids, Val, Ala, and Tyr have a notable β -sheet propensity. For contrast, Leu, known for its

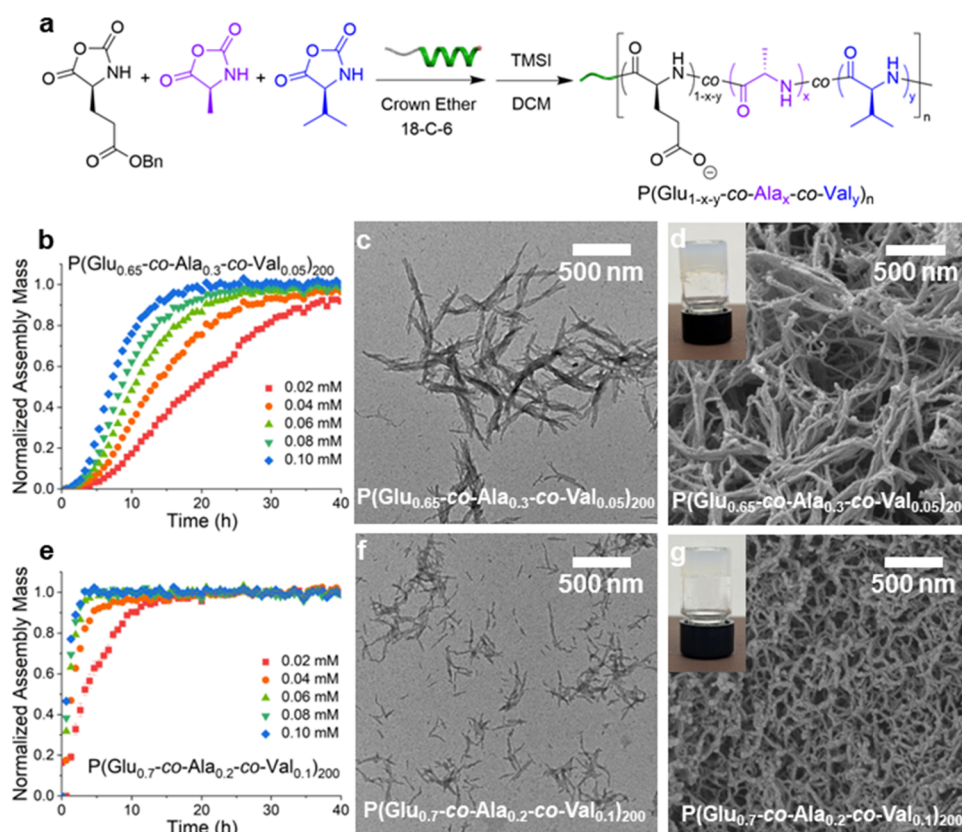


Figure 4. Supramolecular assembly and fibril network of tricomponent copolypeptides $P(\text{Glu}_{1-x-y}\text{-co-Ala}_x\text{-co-Val}_y)_n$. (a) Schematic representation of the synthetic route for $P(\text{Glu}_{1-x-y}\text{-co-Ala}_x\text{-co-Val}_y)_n$. (b, e) Kinetic assembly profiles for $P(\text{Glu}_{0.65}\text{-co-Ala}_{0.3}\text{-co-Val}_{0.05})_{200}$ and $P(\text{Glu}_{0.7}\text{-co-Ala}_{0.2}\text{-co-Val}_{0.1})_{200}$, respectively, at various initial monomer concentrations. (c, f) TEM images of assemblies from $P(\text{Glu}_{0.65}\text{-co-Ala}_{0.3}\text{-co-Val}_{0.05})_{200}$ and $P(\text{Glu}_{0.7}\text{-co-Ala}_{0.2}\text{-co-Val}_{0.1})_{200}$, respectively. (d, g) SEM images of $P(\text{Glu}_{0.65}\text{-co-Ala}_{0.3}\text{-co-Val}_{0.05})_{200}$ and $P(\text{Glu}_{0.7}\text{-co-Ala}_{0.2}\text{-co-Val}_{0.1})_{200}$ hydrogels, respectively, after supercritical CO_2 drying. Inset: photographs of the opaque supramolecular hydrogels concentrated at 20 mg/mL.

propensity to form stable α -helical conformation, was also integrated.^{66–68} Our synthesized series includes $P(\text{Glu}_{1-x}\text{-co-Leu}_x)_{100}$, $P(\text{Glu}_{1-x}\text{-co-Ala}_x)_{100}$, $P(\text{Glu}_{1-x}\text{-co-Val}_x)_{100}$, and $P(\text{Glu}_x\text{-co-Tyr}_{1-x})_n$, with 'x' values ranging between 0.05 to 0.4 (Figure 3a and Figure S4–7). Conformations of the resulting copolypeptides at different pH values were confirmed by CD (Figure S11–14). Given the pronounced hydrophobicity of Leu and Val's side chains,⁶⁹ copolypeptides consisting of more than 15% of these amino acids rapidly segregated into amorphous structures under the assembly conditions. However, both $P(\text{Glu}_{0.9}\text{-co-Leu}_{0.1})_{100}$ and $P(\text{Glu}_{0.9}\text{-co-Val}_{0.1})_{100}$ formed distinct fibril superstructures in the diluted solutions (Figure 3b,d, Figure S25 and S27). Individual fibrils in the bundles can be visualized in the negative stained TEM images (Figure S24). In comparison, $P(\text{Glu}_{1-x}\text{-co-Ala}_x)_{100}$, with Ala compositions of 20% or 30%, produced fibril superstructures (Figure 3c and Figure S26), attributed to the slightly reduced hydrophobic nature of Ala's side chain compared to Leu or Val. These fibrils, especially from $P(\text{Glu}_{0.9}\text{-co-Leu}_{0.1})_{100}$ and $P(\text{Glu}_{0.9}\text{-co-Val}_{0.1})_{100}$, predominantly exhibited a β -sheet secondary structure, as revealed by FTIR and WAXD studies (Figure S18 and S19). In addition to the β -sheet structure, coil conformation was also evident in fibrils from $P(\text{Glu}_{0.8}\text{-co-Ala}_{0.2})_{100}$, with FITR spectra indicating a peak at 1645 cm^{-1} and WAXD profiles lacking the α -helix signature (Figure S18 and S19). In contrast, $P(\text{Glu}_x\text{-co-Tyr}_{1-x})_n$ primarily formed amorphous aggregates in solution, as a result of the strong interactions between aromatic side groups (Figure S28).

$P(\text{Glu}_{0.9}\text{-co-Leu}_{0.1})_{100}$ demonstrated the slowest fibril formation, with the fibrillation following a two-stage, nucleation–growth process that could be accelerated by increasing the polymer concentration (Figure 3e and Figure S25). The kinetics was even slower than that of PGLu, as Leu has a high propensity to form a α -helical conformation, trapping the copolypeptides in the helical state before they convert into β -sheet fibrils. The slowly formed fibrils assembled pairwise into well-ordered bundles, and gelation was not observed, even at saturated concentrations. Ala, considered to be equally adept in forming α -helical and β -sheet structures,^{71,72} influences the fibrillation of $P(\text{Glu}_{0.8}\text{-co-Ala}_{0.2})_{100}$ differently. As shown in Figure 3f and Figure S26, this copolypeptide fibrillated faster than $P(\text{Glu}_{0.9}\text{-co-Leu}_{0.1})_{100}$. The resultant fibrils from $P(\text{Glu}_{0.8}\text{-co-Ala}_{0.2})_{100}$ exhibit a combination of β -sheet and coil structures. Interestingly, the fibrils in the superstructures were considerably loose, presumably because the higher percentage of Ala disrupted the regularity of the fibril interactions. In diluted conditions, the fibrils measured a few microns in length and became even longer when the Ala composition in the copolypeptides increased from 20% to 30% (Figure S26f). However, no gelation was observed, although the suspension became viscous at high polymer concentrations. Val has the strongest β -sheet propensity among the nonpolar amino acids we tested.^{66–68} Similar to Ser, there was almost no lag phase in the fibrillation of $P(\text{Glu}_{0.9}\text{-co-Val}_{0.1})_{100}$ (Figure 3g and Figure S27). Due to the high hydrophobicity of Val, the fibrils formed branched fibril clusters with multiple filaments at

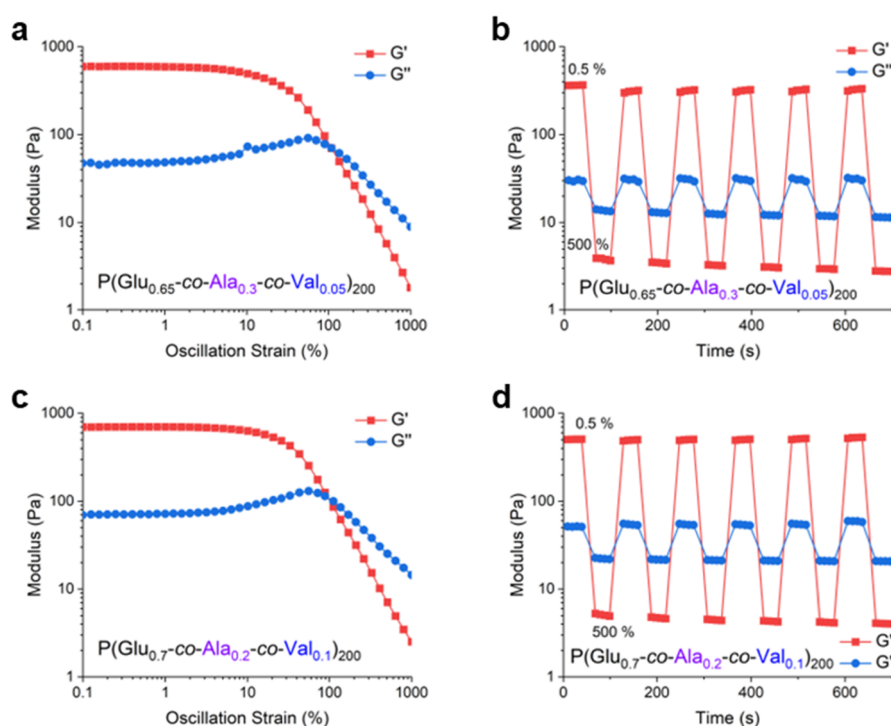


Figure 5. Rheological behavior of hydrogel networks comprising interlinked fibril clusters. (a, c) Strain-dependent oscillatory rheology ($\omega = 1.0$ rad/s, 25 °C) for $P(\text{Glu}_{0.65}\text{-co-Ala}_{0.3}\text{-co-Val}_{0.05})_{200}$ and $P(\text{Glu}_{0.7}\text{-co-Ala}_{0.2}\text{-co-Val}_{0.1})_{200}$ hydrogel, respectively. (b, d) Oscillatory rheology of $P(\text{Glu}_{0.65}\text{-co-Ala}_{0.3}\text{-co-Val}_{0.05})_{200}$ and $P(\text{Glu}_{0.7}\text{-co-Ala}_{0.2}\text{-co-Val}_{0.1})_{200}$ hydrogel, respectively, alternating between 0.5 and 500% strain over 30-s intervals ($\omega = 1.0$ rad/s, 25 °C), demonstrating their self-healing characteristics. Concentration for $P(\text{Glu}_{1-x-y}\text{-co-Ala}_x\text{-co-Val}_y)_{200}$ was set at 20 mg/mL.

a cross-link, but these connected clusters also tended to precipitate under concentrated conditions.

The assembly kinetics were analyzed using established models for protein and amyloid aggregation.^{1,73,74} The time to reach half-completion of fibril assembly (half-time) was determined from the kinetic curves presented in Figure 3e–g. The scaling exponent (γ), which indicates how the half-time varies with the initial copolyptide concentration, was derived from the slopes in Figure 3h–j. The values of these exponents, ranging from -1.1 to -0.8, suggest that secondary nucleation is the predominant mechanism in fibril formation, similar to the aggregation of amyloid- β peptides.^{75,76} The initial growth phase, as well as the entire assembly process, is well-described by a fibril formation model that assumes control by secondary nucleation, with n_2 (the secondary nucleation reaction order with respect to the monomer) being 1, and n_c (the primary nucleation reaction order) being 2 or 3, as detailed in Table S2 and Figure S30. Notably, the inclusion of Val in the copolyptides markedly accelerates both primary and secondary nucleation, thus identifying Val as a potent modulator in the design of a tricomponent system.

To form a stable filament network, semiflexible filaments must exceed a certain density and length for effective percolation through sufficient cross-linking. Moreover, cross-linking must occur rapidly to prevent large filament clusters from precipitating out of the solution. Clearly, the distinct nonpolar amino acids integrated into the copolyptides significantly influenced both the structural morphology and connectivity of the fibril superstructures, as well as the kinetics of their formation. To achieve an effective, sample-spanning network, it is crucial to engineer fibril clusters with both high aspect ratios and robust cross-linking propensities, while also ensuring rapid kinetics throughout the assembly process. With

these criteria in mind, we proposed to combine Ala's fibril-elongating effects with Val's rapid nucleation capabilities to design $P(\text{Glu}_{1-x-y}\text{-co-Ala}_x\text{-co-Val}_y)_n$ copolyptides for realizing the formation of supramolecular filament network.

Tricomponent Copolyptide Assembly into Rigid Branched Fibril Networks. Leveraging on the crown-ether (CE) catalyzed ROP-NCA method we recently developed,⁶³ we synthesized two samples, $P(\text{Glu}_{0.65}\text{-co-Ala}_{0.3}\text{-co-Val}_{0.05})_{200}$ and $P(\text{Glu}_{0.7}\text{-co-Ala}_{0.2}\text{-co-Val}_{0.1})_{200}$, for examination (Figure 4a and Figure S8). Conformations of the resulting copolyptide at different pH values were confirmed by CD (Figure S15). Under diluted conditions, both copolyptides assembled into loose, high-aspect-ratio fibril clusters without experiencing a significant lag phase (Figure 4b,e and Figure S29). Those fibril clusters (Figure 4c,f) were much smaller than those from $P(\text{Glu}_{0.9}\text{-co-Leu}_{0.1})_{100}$, $P(\text{Glu}_{0.8}\text{-co-Ala}_{0.2})_{100}$, and $P(\text{Glu}_{0.9}\text{-co-Val}_{0.1})_{100}$ (Figure 3b–d). When $P(\text{Glu}_{0.65}\text{-co-Ala}_{0.3}\text{-co-Val}_{0.05})_{200}$ was compared with $P(\text{Glu}_{0.7}\text{-co-Ala}_{0.2}\text{-co-Val}_{0.1})_{200}$, the fibrillation process of the latter markedly accelerated. This is presumably due to increased nucleation sites prompted by the higher Val composition, leading to thinner and shorter fibril clusters. In concentrated solutions, supramolecular gelation occurred, forming an intertwined filament network that manifested as an opaque hydrogel (Figure 4d,g). The fibrils within these networks shared a similar width with the fibril clusters found in the diluted suspension. Unlike the entangled fibril networks formed by $P(\text{Glu}_x\text{-co-Ser}_{1-x})_{200}$, the fibril networks created by $P(\text{Glu}_{0.65}\text{-co-Ala}_{0.3}\text{-co-Val}_{0.05})_{200}$ and $P(\text{Glu}_{0.7}\text{-co-Ala}_{0.2}\text{-co-Val}_{0.1})_{200}$ featured a more rigid, with a “bush-like” branching structure characterized by a high level of connectivity between fibrils. The fibrils assembled from $P(\text{Glu}_{0.65}\text{-co-Ala}_{0.3}\text{-co-Val}_{0.05})_{200}$ and $P(\text{Glu}_{0.7}\text{-co-Ala}_{0.2}\text{-co-Val}_{0.1})_{200}$ exhibited a predominant β -sheet secondary structure

with some coil conformation, as revealed by FTIR and WAXD studies (Figure S20 and S21). Observing that the filament density in the $P(\text{Glu}_{0.7}\text{-co-Ala}_{0.2}\text{-co-Val}_{0.1})_{200}$ sample appeared to be higher than that in $P(\text{Glu}_{0.65}\text{-co-Ala}_{0.3}\text{-co-Val}_{0.05})_{200}$, we prepared an additional sample, $P(\text{Glu}_{0.65}\text{-co-Ala}_{0.25}\text{-co-Val}_{0.1})_{200}$. The morphology of its fibril network closely resembled that of $P(\text{Glu}_{0.7}\text{-co-Ala}_{0.2}\text{-co-Val}_{0.1})_{200}$, as shown in Figure S33. This similarity indicates that the filament density in these hydrogel networks is primarily influenced by the composition of Val.

Several factors may contribute to this unique superstructure control: (1) The chain regularity was significantly disrupted by the inclusion of Ala and Val residues, preventing the pairwise stacking of β -sheet protofibrils into large spherulites that are prone to precipitation. (2) The introduction of Val facilitated rapid nucleation, while Ala effectively moderated the growth phase. This synergistic effect led to the formation of fibril bundles that predominantly assembled into branched fibril clusters, swiftly covering the entire sample space. (3) The hydrophobic attractions between the nonpolar residues fostered an increased network connectivity between the fibrils and fibril bundles.

Enhanced Mechanical Strength and Structural Adaptability of Interlinked Fibril Cluster Hydrogels. In comparison with entangled fibril hydrogels from $P(\text{Glu}_{1-x}\text{-co-Ser}_x)_{200}$, the hydrogel composed of $P(\text{Glu}_{0.65}\text{-co-Ala}_{0.3}\text{-co-Val}_{0.05})_{200}$ showed substantially greater strength, reaching a G' of 600 Pa (Figure 5a and Figure S34a). This suggests enhanced stability within the fibril cluster network. The higher hydrophobicity of its amino acid constituents in $P(\text{Glu}_{0.65}\text{-co-Ala}_{0.3}\text{-co-Val}_{0.05})_{200}$ led to stronger chain interactions and increased fibril connectivity, forming a more resilient filament network. Interestingly, while the fibril superstructures of hydrogel of $P(\text{Glu}_{0.7}\text{-co-Ala}_{0.2}\text{-co-Val}_{0.1})_{200}$ were significantly thinner and denser than those of $P(\text{Glu}_{0.65}\text{-co-Ala}_{0.3}\text{-co-Val}_{0.05})_{200}$, their G' and strain-dependence were similar (Figure 5c and Figure S34b). However, the G'' of the $P(\text{Glu}_{0.7}\text{-co-Ala}_{0.2}\text{-co-Val}_{0.1})_{200}$ hydrogel was nearly double that of $P(\text{Glu}_{0.65}\text{-co-Ala}_{0.3}\text{-co-Val}_{0.05})_{200}$. Despite their superior strength, the networks of $P(\text{Glu}_{0.65}\text{-co-Ala}_{0.3}\text{-co-Val}_{0.05})_{200}$ and $P(\text{Glu}_{0.7}\text{-co-Ala}_{0.2}\text{-co-Val}_{0.1})_{200}$ maintained a self-healing capability comparable to that of $P(\text{Glu}_{0.5}\text{-co-Ser}_{0.5})_{200}$ when subjected to large strains (Figure 5b,d).

While the structural aspects in these fibril cluster gels might resemble those found in some rod cluster gels formed in colloidal assembly,⁴² they are not premade building blocks assembled later by depletion forces. Instead, the copolypeptides, functioning as supramolecular monomers, gradually evolved into an interconnected fibril cluster network. This fibril nucleation and growth persist until the entire available space is filled by the connected supramolecular network, arresting the dynamics of individual fibrils or fibril clusters. This gelation process is strongly governed by supramolecular assembly kinetics, making them highly responsive to variations in molecular designs. For example, with 5% Val percentage, resulting filaments from $P(\text{Glu}_{0.65}\text{-co-Ala}_{0.3}\text{-co-Val}_{0.05})_{200}$ tend to be elongated and thick, albeit at a reduced filament density. In contrast, with 10% Val, enhanced nucleation amplifies filament density, producing shorter, finer filaments in the $P(\text{Glu}_{0.7}\text{-co-Ala}_{0.2}\text{-co-Val}_{0.1})_{200}$ hydrogel, given the same polypeptide concentration. For filaments of a given range of persistence lengths, the elasticity of semiflexible filament networks is typically a function of filament length and density.¹⁵ Longer filaments with lower densities might

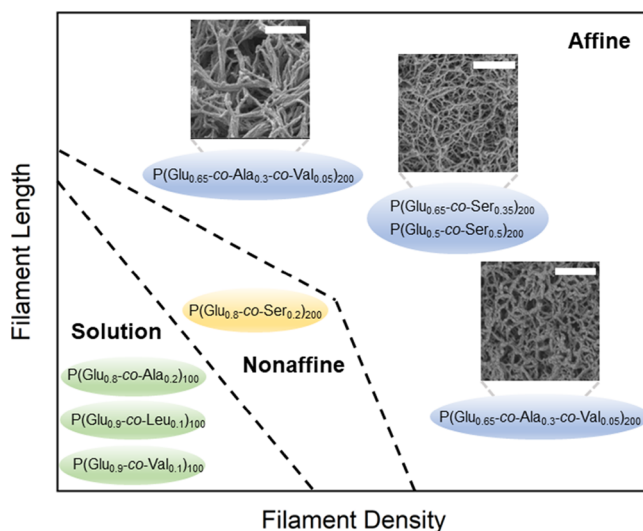
emphasize the entropic stretching of filaments for elasticity. Meanwhile, shorter, denser filaments might shift the network's dominance to enthalpic bending and stretching.⁶⁷ Our random copolypeptides offer a diverse range of filament lengths, densities, and connectivities, creating experimental model systems to explore the physics of such networks.

General Design Concepts for Fibrous Networks Derived from Synthetic Random Copolypeptides.

Macintosh and colleagues have previously developed a diagram that illustrates how variations in the length and number density of semiflexible filaments influence network elasticity.^{15,77} This diagram offers a clear depiction of the network behavior, making it a valuable tool in guiding the experimental design of a fibrous network. For example, short filaments at low densities are insufficient for forming networks due to inadequate cross-linking, which leaves the filaments in a solute state. Beyond a certain threshold of density and length, a percolation network forms, yet it may display nonaffine characteristics where local regions deform independently of the overall macroscopic deformation. In contrast, networks composed of long filaments at low densities, or those with high densities but short intercross-link filament lengths, tend to exhibit affine behavior. Here, local deformations are coordinated with the macroscopic strain, leading to distinctive elastic and mechanical properties.

In our study, the dynamics of filament network and the nature of cross-links are also crucial, considering that the cross-links between filaments in supramolecular gels may be transient. Yet qualitatively, the behaviors of fibrils or fibril networks derived from specific copolypeptide compositions align with the regions outlined in Scheme 2, conforming to the

Scheme 2. Sketch Representation of a Diagram Categorizing Filamentous Assemblies or Networks Formed by Synthetic Copolypeptides with Specific Compositions (Scale Bar: 500 nm)



general trends of length and density dependence described by the established theory.⁷⁷ Although our findings are still in their early stages, this dependence could inform the design of copolypeptides for specific network architectures. It is remarkable that our investigations, using a limited set of just five amino acids, have yielded a diverse array of network structures. Nevertheless, additional studies are necessary to definitively categorize these structures within the distinct

regimes of affine or nonaffine networks, based on their elastic responses and deformation modes—whether filaments predominantly stretch and compress or bending modes prevail.¹⁵ Furthermore, our hydrogel samples exhibited a broad spectrum of storage and loss moduli, without relying on non-network species, external modulators, or added cross-linkers. These moduli values are comparable to those found in reconstituted extracellular matrices (ECM),^{7,14} e.g., G' : 10–1000 Pa; G'' : 1–100 Pa. We anticipate that the introduction of permanent cross-links, such as by integrating a minor proportion of cysteine (Cys) into the random copolypeptides, could markedly enhance the modulus, bringing it closer to the viscoelastic properties of soft tissues.

CONCLUSIONS

In summary, this study presents two novel strategies for the design and synthesis of synthetic random copolypeptides with the potential to self-assemble into biomimetic supramolecular hydrogels. The first approach utilizes amino acids with polar side chains, specifically serine, to develop copolypeptides that can form stable filament networks with tunable viscoelastic properties. The second strategy employs nonpolar amino acids, specifically valine and alanine, harnessing their ability to steer the architecture of fibrils, influencing their higher-order superstructures and assembly kinetics and thus promoting the creation of extensive networks. Both strategies yielded supramolecular hydrogels characterized by a self-healing capability, underscoring their potential suitability for biomedical applications. Furthermore, this work sheds light on the core principles steering the gelation pathways of synthetic copolypeptides, enhancing our understanding of the intrinsic processes that guide their self-assembling tendencies. Future research could seek to broaden this knowledge base, exploring diverse amino acid combinations and their synergistic actions to refine the tunability of mechanical and other physical properties in these synthetic filamentary networks.

ASSOCIATED CONTENT

Supporting Information

The Supporting Information is available free of charge at <https://pubs.acs.org/doi/10.1021/jacs.3c10762>.

Materials and methods; nuclear magnetic resonance (NMR); gel permeation chromatography (GPC); NCA copolymerization kinetics by high performance liquid chromatography (HPLC); circular dichroism (CD) spectra; Fourier transform infrared (FTIR) spectra; small-angle X-ray scattering (SAXS) and wide-angle X-ray scattering (WAXS); ThT-based fluorescence kinetic assays by microplate reader; transmission electron microscopy (TEM) and negatively stained TEM; Scanning electron microscopy (SEM) and critical point dryer; rheology; experimental section; synthesis of *O*-benzyl-L-Serine NCA (BLS-NCA); synthesis of *O*-benzyl-L-tyrosine NCA (BLT-NCA); synthesis of copolypeptides with leucine, alanine, valine, and tyrosine; synthesis of copolypeptides with serine via SIMPLE polymerization method; synthesis of copolypeptides with three components with crown ether (CE) as catalyst; determination of the randomness of amino acids in the copolypeptides by NCA ROP copolymerization kinetics; supramolecular assembly of copolypeptides in dilute solutions; supramolecular hydrogelation of

copolypeptides; supramolecular assembly kinetics of copolypeptides monitored by *in situ* ThT fluorescence assays; supramolecular assembly kinetic data processing; analysis of the supramolecular assembly kinetics; statistics of the length and width of supramolecular assemblies (PDF)

AUTHOR INFORMATION

Corresponding Authors

Jianjun Cheng – Department of Chemistry and Department of Materials Science and Engineering, University of Illinois at Urbana–Champaign, Urbana, Illinois 61801, United States; orcid.org/0000-0003-2561-9291; Email: jianjunc@illinois.edu

Yao Lin – Polymer Program, Institute of Materials Science and Department of Chemistry, University of Connecticut, Storrs, Connecticut 06269, United States; orcid.org/0000-0001-5227-2663; Email: yao.lin@uconn.edu

Authors

Tianjian Yang – Polymer Program, Institute of Materials Science, University of Connecticut, Storrs, Connecticut 06269, United States

Tianrui Xue – Department of Chemistry, University of Illinois at Urbana–Champaign, Urbana, Illinois 61801, United States

Jianan Mao – Department of Chemistry, University of Connecticut, Storrs, Connecticut 06269, United States

Yingying Chen – Department of Materials Science and Engineering, University of Illinois at Urbana–Champaign, Urbana, Illinois 61801, United States

Huidi Tian – Department of Chemistry, University of Connecticut, Storrs, Connecticut 06269, United States

Arlene Bartolome – Department of Chemistry, University of Connecticut, Storrs, Connecticut 06269, United States

Hongwei Xia – Department of Chemistry, University of Connecticut, Storrs, Connecticut 06269, United States

Xudong Yao – Department of Chemistry, University of Connecticut, Storrs, Connecticut 06269, United States

Challa V. Kumar – Department of Chemistry, University of Connecticut, Storrs, Connecticut 06269, United States; orcid.org/0000-0002-4396-8738

Complete contact information is available at: <https://pubs.acs.org/doi/10.1021/jacs.3c10762>

Author Contributions

[†]T.Y. and T.X. contributed equally to this work.

Notes

The authors declare no competing financial interest.

ACKNOWLEDGMENTS

This work was supported by the NSF grant (DMR 1809497 and DMR 2210590 to Y.L.; CHE-1905097 to J.C.). The authors thank Dr. Xuanhao Sun at the UConn Bioscience Electron Microscopy Lab for instrument training, Prof. Anson Ma at the UConn Polymer Program for comments and suggestions, and Dr. Lin Yang at the Brookhaven National Lab for assistance with WAXD studies. The LiX beamline is part of the Center for BioMolecular Structure (CBMS), which is primarily supported by the National Institutes of Health, National Institute of General Medical Sciences (NIGMS) through a P30 Grant (P30GM133893), and by the DOE

Office of Biological and Environmental Research (KP1605010). LiX also received additional support from NIH Grant S10 OD012331. As part of NSLS-II, a national user facility at Brookhaven National Laboratory, work performed at the CBMS is supported in part by the U.S. Department of Energy, Office of Science, Office of Basic Energy Sciences Program under contract number DE-SC0012704.

REFERENCES

- (1) Oosawa, F.; Asakura, S. *Thermodynamics of the Polymerization of Protein*; Academic Press, 1975.
- (2) Fletcher, D. A.; Mullins, R. D. Cell mechanics and the cytoskeleton. *Nature* **2010**, *463*, 485–492.
- (3) Pollard, T. D.; Borisy, G. G. Cellular motility driven by assembly and disassembly of actin filaments. *Cell* **2003**, *112*, 453–465.
- (4) Goodwin, S. S.; Vale, R. D. Patronin regulates the microtubule network by protecting microtubule minus ends. *Cell* **2010**, *143*, 263–274.
- (5) Yurchenco, P. D.; Ruben, G. C. Basement membrane structure in situ: evidence for lateral associations in the type IV collagen network. *J. Cell Biol.* **1987**, *105*, 2559–2568.
- (6) Ottani, V.; Raspanti, M.; Ruggeri, A. Collagen structure and functional implications. *Micron* **2001**, *32*, 251–260.
- (7) Storm, C.; Pastore, J. J.; MacKintosh, F. C.; Lubensky, T. C.; Janmey, P. A. Nonlinear elasticity in biological gels. *Nature* **2005**, *435*, 191–194.
- (8) Gardel, M.; Shin, J. H.; MacKintosh, F.; Mahadevan, L.; Matsudaira, P.; Weitz, D. A. Elastic behavior of cross-linked and bundled actin networks. *Science* **2004**, *304*, 1301–1305.
- (9) Lin, Y.-C.; Koenderink, G. H.; MacKintosh, F. C.; Weitz, D. A. Viscoelastic properties of microtubule networks. *Macromolecules* **2007**, *40*, 7714–7720.
- (10) Forgacs, G.; Newman, S. A.; Hinner, B.; Maier, C. W.; Sackmann, E. Assembly of collagen matrices as a phase transition revealed by structural and rheologic studies. *Biophys. J.* **2003**, *84*, 1272–1280.
- (11) Licup, A. J.; Münster, S.; Sharma, A.; Sheinman, M.; Jawerth, L. M.; Fabry, B.; Weitz, D. A.; MacKintosh, F. C. Stress controls the mechanics of collagen networks. *Proc. Natl. Acad. Sci. U. S. A.* **2015**, *112*, 9573–9578.
- (12) Fratzl, P.; Misof, K.; Zizak, I.; Rapp, G.; Amenitsch, H.; Bernstorff, S. Fibrillar structure and mechanical properties of collagen. *J. Struct. Biol.* **1998**, *122*, 119–122.
- (13) Moendarbary, E.; Valon, L.; Fritzsche, M.; Harris, A. R.; Moulding, D. A.; Thrasher, A. J.; Stride, E.; Mahadevan, L.; Charras, G. T. The cytoplasm of living cells behaves as a poroelastic material. *Nat. Mater.* **2013**, *12*, 253–261.
- (14) Chaudhuri, O.; Cooper-White, J.; Janmey, P. A.; Mooney, D. J.; Shenoy, V. B. Effects of extracellular matrix viscoelasticity on cellular behaviour. *Nature* **2020**, *584*, 535–546.
- (15) Pritchard, R. H.; Huang, Y. Y. S.; Terentjev, E. M. Mechanics of biological networks: from the cell cytoskeleton to connective tissue. *Soft Matter* **2014**, *10*, 1864–1884.
- (16) Yokoi, H.; Kinoshita, T.; Zhang, S. Dynamic reassembly of peptide RADA16 nanofiber scaffold. *Proc. Natl. Acad. Sci. U. S. A.* **2005**, *102*, 8414–8419.
- (17) Li, X.; Kuang, Y.; Lin, H. C.; Gao, Y.; Shi, J.; Xu, B. Supramolecular nanofibers and hydrogels of nucleopeptides. *Angew. Chem., Int. Ed.* **2011**, *50*, 9365–9369.
- (18) Freeman, R.; Han, M.; Álvarez, Z.; Lewis, J. A.; Wester, J. R.; Stephanopoulos, N.; McClendon, M. T.; Lynsky, C.; Godbe, J. M.; Sangji, H.; Luijten, E.; Stupp, S. I. Reversible self-assembly of superstructured networks. *Science* **2018**, *362*, 808–813.
- (19) Kouwer, P. H.; Koepf, M.; Le Sage, V. A.; Jaspers, M.; Van Buul, A. M.; Eksteen-Akeroyd, Z. H.; Woltinge, T.; Schwartz, E.; Kitto, H. J.; Hoogenboom, R.; Picken, S. J.; Nolte, R. J. M.; Mendes, E.; Rowan, A. E. Responsive biomimetic networks from polyisocyanopeptide hydrogels. *Nature* **2013**, *493*, 651–655.
- (20) O’leary, L. E.; Fallas, J. A.; Bakota, E. L.; Kang, M. K.; Hartgerink, J. D. Multi-hierarchical self-assembly of a collagen mimetic peptide from triple helix to nanofiber and hydrogel. *Nat. Chem.* **2011**, *3*, 821–828.
- (21) Wang, F.; Su, H.; Xu, D.; Dai, W.; Zhang, W.; Wang, Z.; Anderson, C. F.; Zheng, M.; Oh, R.; Wan, F.; Cui, H. Tumour sensitization via the extended intratumoural release of a STING agonist and camptothecin from a self-assembled hydrogel. *Nat. Biomed. Eng.* **2020**, *4*, 1090–1101.
- (22) Diba, M.; Spaans, S.; Hendrikse, S. I. S.; Bastings, M. M. C.; Schotman, M. J. G.; van Sprang, J. F.; Wu, D. J.; Hoebe, F. J. M.; Janssen, H. M.; Dankers, P. Y. W. Engineering the dynamics of cell adhesion cues in supramolecular hydrogels for facile control over cell encapsulation and behavior. *Adv. Mater.* **2021**, *33*, 2008111.
- (23) Chivers, P. R.; Smith, D. K. Shaping and structuring supramolecular gels. *Nat. Rev. Mater.* **2019**, *4*, 463–478.
- (24) Gelain, F.; Luo, Z.; Zhang, S. Self-assembling peptide EAK16 and RADA16 nanofiber scaffold hydrogel. *Chem. Rev.* **2020**, *120*, 13434–13460.
- (25) Petka, W. A.; Harden, J. L.; McGrath, K. P.; Wirtz, D.; Tirrell, D. A. Reversible hydrogels from self-assembling artificial proteins. *Science* **1998**, *281*, 389–392.
- (26) van Hest, J. C.; Tirrell, D. A. Protein-based materials, toward a new level of structural control. *Chem. Commun.* **2001**, 1897–1904.
- (27) Vepari, C.; Kaplan, D. L. Silk as a biomaterial. *Prog. Polym. Sci.* **2007**, *32*, 991–1007.
- (28) Levin, A.; Hakala, T. A.; Schnaider, L.; Bernardes, G. J. L.; Gazit, E.; Knowles, T. P. J. Biomimetic peptide self-assembly for functional materials. *Nat. Rev. Chem.* **2020**, *4*, 615–634.
- (29) Deng, C.; Wu, J.; Cheng, R.; Meng, F.; Klok, H.-A.; Zhong, Z. Functional polypeptide and hybrid materials: Precision synthesis via α -amino acid N-carboxyanhydride polymerization and emerging biomedical applications. *Prog. Polym. Sci.* **2014**, *39*, 330–364.
- (30) Deming, T. J. Synthetic polypeptides for biomedical applications. *Prog. Polym. Sci.* **2007**, *32*, 858–875.
- (31) Hadjichristidis, N.; Iatrou, H.; Pitsikalis, M.; Sakellariou, G. Synthesis of well-defined polypeptide-based materials via the ring-opening polymerization of α -amino acid N-carboxyanhydrides. *Chem. Rev.* **2009**, *109*, 5528–5578.
- (32) Deming, T. J. Synthesis of side-chain modified polypeptides. *Chem. Rev.* **2016**, *116*, 786–808.
- (33) Lu, H.; Wang, J.; Song, Z.; Yin, L.; Zhang, Y.; Tang, H.; Tu, C.; Lin, Y.; Cheng, J. Recent advances in amino acid N-carboxyanhydrides and synthetic polypeptides: chemistry, self-assembly and biological applications. *Chem. Commun.* **2014**, *50*, 139–155.
- (34) Rodríguez-Hernández, J.; Chécot, F.; Gnanou, Y.; Lecommandoux, S. Toward ‘smart’ nano-objects by self-assembly of block copolymers in solution. *Prog. Polym. Sci.* **2005**, *30*, 691–724.
- (35) Chen, S.; Berthelot, V.; Hamilton, J. B.; O’Nuallai, B.; Wetzel, R. Amyloid-like features of polyglutamine aggregates and their assembly kinetics. *Biochem. J.* **2002**, *41*, 7391–7399.
- (36) Fändrich, M.; Dobson, C. M. The behaviour of polyamino acids reveals an inverse side chain effect in amyloid structure formation. *EMBO J.* **2002**, *21*, 5682–5690.
- (37) Yang, T.; Benson, K.; Fu, H.; Xue, T.; Song, Z.; Duan, H.; Xia, H.; Kalluri, A.; He, J.; Cheng, J.; Kumar, C. V.; Lin, Y. Modeling and Designing Particle-Regulated Amyloid-like Assembly of Synthetic Polypeptides in Aqueous Solution. *Biomacromolecules* **2021**, *23*, 196–209.
- (38) Colaco, M.; Park, J.; Blanch, H. The kinetics of aggregation of poly-glutamic acid based polypeptides. *Biophys. Chem.* **2008**, *136*, 74–86.
- (39) Du, X.; Zhou, J.; Shi, J.; Xu, B. Supramolecular hydrogelators and hydrogels: from soft matter to molecular biomaterials. *Chem. Rev.* **2015**, *115*, 13165–13307.
- (40) Goor, O. J.; Hendrikse, S. I.; Dankers, P. Y.; Meijer, E. From supramolecular polymers to multi-component biomaterials. *Chem. Soc. Rev.* **2017**, *46*, 6621–6637.

- (41) Mohraz, A.; Solomon, M. J. Gelation and internal dynamics of colloidal rod aggregates. *J. Colloid Interface Sci.* **2006**, *300*, 155–162.
- (42) Wilkins, G. M.; Spicer, P. T.; Solomon, M. J. Colloidal systems to explore structural and dynamical transitions in rod networks, gels, and glasses. *Langmuir* **2009**, *25*, 8951–8959.
- (43) Meakin, P. *Fractals, scaling and growth far from equilibrium*; Cambridge University Press, 1998.
- (44) Trappe, V.; Prasad, V.; Cipelletti, L.; Segre, P.; Weitz, D. A. Jamming phase diagram for attractive particles. *Nature* **2001**, *411*, 772–775.
- (45) Solomon, M. J.; Spicer, P. T. Microstructural regimes of colloidal rod suspensions, gels, and glasses. *Soft Matter* **2010**, *6*, 1391–1400.
- (46) Su, L.; Mosquera, J.; Mabesoone, M. F.; Schoenmakers, S. M.; Muller, C.; Vleugels, M. E.; Dhiman, S.; Wijker, S.; Palmans, A. R.; Meijer, E. Dilution-induced gel-sol-gel-sol transitions by competitive supramolecular pathways in water. *Science* **2022**, *377*, 213–218.
- (47) Pashuck, E. T.; Cui, H.; Stupp, S. I. Tuning supramolecular rigidity of peptide fibers through molecular structure. *J. Am. Chem. Soc.* **2010**, *132*, 6041–6046.
- (48) Edelbrock, A. N.; Clemons, T. D.; Chin, S. M.; Roan, J. J. W.; Bruckner, E. P.; Alvarez, Z.; Edelbrock, J. F.; Wek, K. S.; Stupp, S. I. Superstructured Biomaterials Formed by Exchange Dynamics and Host–Guest Interactions in Supramolecular Polymers. *Adv. Sci.* **2021**, *8*, No. 2004042.
- (49) Xia, H.; Fu, H.; Zhang, Y.; Shih, K.-C.; Ren, Y.; Anuganti, M.; Nieh, M.-P.; Cheng, J.; Lin, Y. Supramolecular assembly of comb-like macromolecules induced by chemical reactions that modulate the macromolecular interactions in situ. *J. Am. Chem. Soc.* **2017**, *139*, 11106–11116.
- (50) Link, A. J.; Mock, M. L.; Tirrell, D. A. Non-canonical amino acids in protein engineering. *Curr. Opin. Biotechnol.* **2003**, *14*, 603–609.
- (51) Liu, C. C.; Schultz, P. G. Adding new chemistries to the genetic code. *Annu. Rev. Biochem.* **2010**, *79*, 413–444.
- (52) Baumgartner, R.; Fu, H.; Song, Z.; Lin, Y.; Cheng, J. Cooperative polymerization of α -helices induced by macromolecular architecture. *Nat. Chem.* **2017**, *9*, 614–622.
- (53) Song, Z.; Fu, H.; Wang, J.; Hui, J.; Xue, T.; Pacheco, L. A.; Yan, H.; Baumgartner, R.; Wang, Z.; Xia, Y.; Wang, X.; Yin, L.; Chen, C.; Rodríguez-López, J.; Ferguson, A. L.; Lin, Y.; Cheng, J. Synthesis of polypeptides via bioinspired polymerization of in situ purified N-carboxyanhydrides. *Proc. Natl. Acad. Sci. U. S. A.* **2019**, *116*, 10658–10663.
- (54) Wang, W.; Fu, H.; Lin, Y.; Cheng, J.; Song, Z. Cooperative Covalent Polymerization of N-carboxyanhydrides: from Kinetic Studies to Efficient Synthesis of Polypeptide Materials. *Acc. Chem. Res.* **2023**, *4*, 604–615.
- (55) Canning, A.; Pasquazi, A.; Fijten, M.; Rajput, S.; Buttery, L.; Aylott, J. W.; Zelzer, M. Tuning the conformation of synthetic copolypeptides of serine and glutamic acid through control over polymer composition. *J. Polym. Sci., Part A: Polym. Chem.* **2016**, *54*, 2331–2336.
- (56) Gibson, M. I.; Cameron, N. R. Organogelation of sheet–helix diblock copolypeptides. *Angew. Chem., Int. Ed.* **2008**, *120*, S238–S240.
- (57) Fan, J.; Zou, J.; He, X.; Zhang, F.; Zhang, S.; Raymond, J. E.; Wooley, K. L. Tunable mechano-responsive organogels by ring-opening copolymerizations of N-carboxyanhydrides. *Chem. Sci.* **2014**, *5*, 141–150.
- (58) Nisal, R.; Jayakannan, M. Tertiary-Butylbenzene Functionalization as a Strategy for β -Sheet Polypeptides. *Biomacromolecules* **2022**, *23*, 2667–2684.
- (59) Xue, T.; Song, Z.; Wang, Y.; Zhu, B.; Zhao, Z.; Tan, Z.; Wang, X.; Xia, Y.; Cheng, J. Streamlined synthesis of PEG-polypeptides directly from amino acids. *Macromolecules* **2020**, *53*, 6589–6597.
- (60) Lu, H.; Cheng, J. Hexamethyldisilazane-mediated controlled polymerization of α -amino acid N-carboxyanhydrides. *J. Am. Chem. Soc.* **2007**, *129*, 14114–14115.
- (61) Song, Z.; Fu, H.; Baumgartner, R.; Zhu, L.; Shih, K.-C.; Xia, Y.; Zheng, X.; Yin, L.; Chipot, C.; Lin, Y.; Cheng, J. Enzyme-mimetic self-catalyzed polymerization of polypeptide helices. *Nat. Commun.* **2019**, *10*, 5470.
- (62) Fu, H.; Baumgartner, R.; Song, Z.; Chen, C.; Cheng, J.; Lin, Y. Generalized model of cooperative covalent polymerization: connecting the supramolecular binding interactions with the catalytic behavior. *Macromolecules* **2022**, *55*, 2041–2050.
- (63) Xia, Y.; Song, Z.; Tan, Z.; Xue, T.; Wei, S.; Zhu, L.; Yang, Y.; Fu, H.; Jiang, Y.; Lin, Y.; Lu, Y.; Ferguson, A. L.; Cheng, J. Accelerated polymerization of N-carboxyanhydrides catalyzed by crown ether. *Nat. Commun.* **2021**, *12*, 732.
- (64) Wang, J.; Lu, H.; Kamat, R.; Pingali, S. V.; Urban, V. S.; Cheng, J.; Lin, Y. Supramolecular polymerization from polypeptide-grafted comb polymers. *J. Am. Chem. Soc.* **2011**, *133*, 12906–12909.
- (65) Quadrioglio, F.; Urry, D. Ultraviolet rotatory properties of polypeptides in solution. II. Poly-L-serine. *J. Am. Chem. Soc.* **1968**, *90*, 2760–2765.
- (66) Koenig, J.; Sutton, P. Raman scattering of some synthetic polypeptides: Poly (γ -benzyl L-glutamate), poly-L-leucine, poly-L-valine, and poly-L-serine. *Biopolymers* **1971**, *10*, 89–106.
- (67) Minor, D. L., Jr; Kim, P. S. Measurement of the β -sheet-forming propensities of amino acids. *Nature* **1994**, *367*, 660–663.
- (68) Levitt, M. Conformational preferences of amino acids in globular proteins. *Biochem.* **1978**, *17*, 4277–4285.
- (69) Sereda, T. J.; Mant, C. T.; Sönnichsen, F. D.; Hodges, R. S. Reversed-phase chromatography of synthetic amphipathic α -helical peptides as a model for ligand/receptor interactions Effect of changing hydrophobic environment on the relative hydrophilicity/hydrophobicity of amino acid side-chains. *J. Chromatogr. A* **1994**, *676*, 139–153.
- (70) Naiki, H.; Higuchi, K.; Hosokawa, M.; Takeda, T. Fluorometric determination of amyloid fibrils in vitro using the fluorescent dye, thioflavine T. *Anal. Biochem.* **1989**, *177*, 244–249.
- (71) Kricheldorf, H. R.; von Lossow, C.; Schwarz, G. Primary Amine-Initiated Polymerizations of Alanine-NCA and Sarcosine-NCA. *Macromol. Chem. Phys.* **2004**, *205*, 918–924.
- (72) Bamford, C. H. *Synthetic Polypeptides: Preparation, Structure, and Properties*; Academic Press, 1956.
- (73) Bishop, M. F.; Ferrone, F. A. Kinetics of nucleation-controlled polymerization. A perturbation treatment for use with a secondary pathway. *Biophys. J.* **1984**, *46*, 631–644.
- (74) Dear, A. J.; Meisl, G.; Michaels, T. C. T.; Zimmermann, M. R.; Linse, S.; Knowles, T. P. J. The catalytic nature of protein aggregation. *J. Chem. Phys.* **2020**, *152*, No. 045101.
- (75) Cohen, S. I.; Linse, S.; Luheshi, L. M.; Hellstrand, E.; White, D. A.; Rajah, L.; Otzen, D. E.; Vendruscolo, M.; Dobson, C. M.; Knowles, T. P. Proliferation of amyloid- β 42 aggregates occurs through a secondary nucleation mechanism. *Proc. Natl. Acad. Sci. U. S. A.* **2013**, *110*, 9758–9763.
- (76) Meisl, G.; Kirkegaard, J. B.; Arosio, P.; Michaels, T. C.; Vendruscolo, M.; Dobson, C. M.; Linse, S.; Knowles, T. P. Molecular mechanisms of protein aggregation from global fitting of kinetic models. *Nat. Protoc.* **2016**, *11*, 252–272.
- (77) Head, D.; Levine, A.; MacKintosh, F. Distinct regimes of elastic response and deformation modes of cross-linked cytoskeletal and semiflexible polymer networks. *Phys. Rev. E* **2003**, *68*, No. 061907.